Advanced multi-source converters for DC microgrids: integrating photovoltaic, wind, and hybrid storage systems

Suganthi Neelagiri, Pasumarthi Usha
Department of Electrical and Electronics Engineering, Dayananda Sagar College of Engineering,
Visveswaraya Technological University, Bangalore, India

Article Info

ABSTRACT

This paper presents a new configuration for integrating multi-source and hybrid energy storage (HES) systems tailored for a direct current (DC) microgrid. Unlike conventional multi-input converters, the proposed design features a hybrid energy storage system combining ultracapacitors and batteries. The proposed system is intended to effectively manage power variations from wind, photovoltaic (PV) sources, and abrupt load changes. The inclusion of ultracapacitors addresses high-frequency fluctuations, thereby extending battery life and reducing the overall size of the storage unit. The control framework is designed to maintain power balance within the system, ensuring that renewable energy sources operate at their maximum power points and that energy storage is efficiently charged and discharged based on power availability. The main advantages of this configuration include: i) a reduced number of switches, ii) built-in voltage boosting and regulation for the ultracapacitor, and power-sharing between the battery and ultracapacitor, and iii) a streamlined control system with fewer components. The paper details the investigation, modeling, and design of the planned system, supported by MATLAB simulation results.

This is an open access article under the [CC BY-SA](#) license.

Corresponding Author:

Suganthi Neelagiri
Department Electrical and Electronics Engineering, Dayananda Sagar College of Engineering
Visveswaraya Technological University
Shavige Malleswara Hills, Kumaraswamy Layout, Bangalore 560078, India
Email: suganthi_neelagiri@yahoo.com

1. INTRODUCTION

The increasing global requirement for energy, coupled with the pressing need to address climate change, highlights the necessity of shifting towards renewable energy sources (RES) for power generation. Traditionally, fossil fuels have been the main energy source [1]. However, these fuels are finite, environmentally harmful, and major contributors to greenhouse gas emissions. As the world confronts the negative impacts of climate change: global warming, calamities, and disruptions to ecosystems, the need for cleaner and more sustainable energy alternatives becomes increasingly need of the hour. Renewable energy sources present a promising solution to these challenges [2]. These energy sources are abundant, can be replenished naturally, and have minimal environmental impact. Transitioning to renewable energy not only helps reduce carbon emissions but also enhances energy security, leads to economic development, and creates employment opportunities in developing green industries [3].

Adopting renewable energy for power generation is a vital step toward a sustainable future, supporting global efforts to mitigate climate change and decrease reliance on finite fossil fuel resources [4]. However, this transition requires significant investment in technology, infrastructure, and policy frameworks to ensure a reliable, affordable, and equitable energy supply for everyone [5]. Wind and solar energy sources

are vital for the development and operation of microgrids, which are localized energy systems that can function independently or alongside the main grid. Designed for flexibility, microgrids are well-suited for integrating RES like wind and solar, as they enhance energy security, sustainability, and resilience [6]. Both wind and solar power are sustainable because they depend on natural, inexhaustible resources. Unlike fossil fuels, they do not emit harmful pollutants or contribute to air pollution. By incorporating wind and solar energy into microgrids, communities and industries can considerably decrease their carbon footprint and contribute to worldwide efforts to tackle climate change. However, due to their intermittent nature, these sources require effective strategies to ensure reliable operation. Photovoltaic (PV) and wind energy are complementary, which helps to mitigate long-term intermittency [7]. However, this complementarity can worsen short-term power fluctuations, leading to increased stress on battery storage systems and potentially larger sizing requirements. Additionally, the lifespan of batteries can be adversely affected [8]. To address these challenges, combining batteries with ultracapacitors in a hybrid energy storage system (HESS) can help reduce battery degradation and minimize storage size. In the proposed microgrid structure, Lithium-ion battery is utilized due to high energy density, and the comparison table of lithium-ion with other batteries is given in Table 1 [9]. Moreover, since PV, wind, and storage units generally operate at lower voltages, voltage boosting is necessary. This underscores the need for appropriate converter arrangements and control systems for effectively integrating HESS with renewable power sources. Existing research has discovered several configurations for interfacing battery-ultracapacitor-based HESS [10], [11], as illustrated in Figure 1.
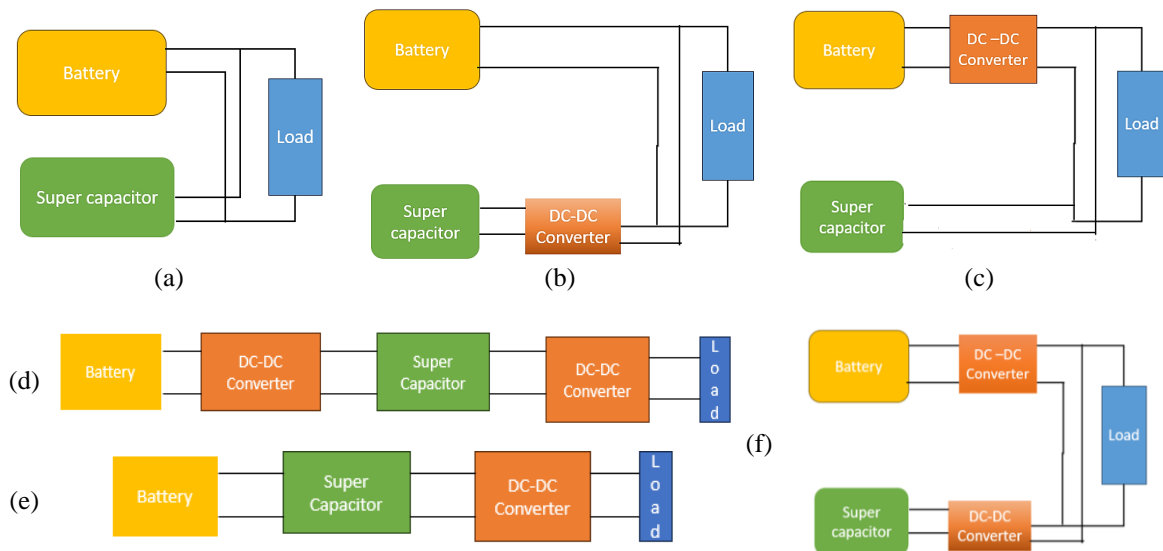

Figure 1. Different HESS configurations: (a) passive configuration, (b) semi-active configuration,
(c) semi-active configuration, (d) fully active configuration with two DC-DC converters,
(e) fully active series configuration, and (f) active parallel configuration

In Figure 1(a), a passive HESS configuration is shown, in which both the battery and the ultracapacitor are directly linked to the load. While this setup is cost-effective and straightforward, it suffers from poor volumetric efficiency and lacks the ability to handle transient power sharing effectively. Furthermore, matching the voltage ratings of the battery and ultracapacitor to the DC link voltage complicates the sizing of the HESS. The semi-active HESS topologies in Figure 1(b) and Figure 1(c) offer improvements over the passive connection. In the above-mentioned topologies, either the battery or the ultracapacitor is linked to the load through a DC-DC converter. Although these configurations address some limitations of the passive setup, they have their issues. For instance, Figure 1(b) may lead to reduced battery life due to high-frequency currents, while Figure 1(c) can experience challenges such as the linear charging/discharging features of the ultracapacitor, reduced volumetric efficiency, and the essential for a larger ultracapacitor.

Fully active configurations, depicted in Figures 1(d)-1(f), use DC-DC converters to interface both the battery and ultracapacitor. These configurations help to overcome issues related to volumetric efficiency and control. However, they face difficulties such as managing the broad operational voltage range of ultracapacitors, suboptimal momentary power allocation between the battery and ultracapacitor, and increased ripple currents affecting the battery. The active parallel HESS configuration shown in Figure 1(f) addresses many of these problems but requires dedicated converters and a more complex control system.

In microgrid applications, the arrangement depicted in Figure 1(f) is often implemented. In this proposed microgrid system, energy storage devices play a vital role, especially batteries [12]. The standard microgrid setup is given in Figure 2, which consists of PV and wind as the main energy sources and battery and ultracapacitor as HESS. All these energy sources and energy storage devices are connected to a common DC bus via appropriate converters. Previous research [13]-[16] has utilized similar configurations, achieving notable improvements in system performance, efficient power delivery, and enhanced usage of ultracapacitors. However, these configurations typically involve dedicated converters [16]-[27], which can lead to increased system costs, higher power losses, complex control systems, a greater number of sensors, and reduced reliability. Additionally, because the ultracapacitor is only active during sudden disturbances, its associated converter often remains idle.

Table 1. Different battery performance comparison

| Technology	Energy Density (Wh/kg)	Cycle Life	Charge Time	Operating Temperature	Cost	Advantages	Disadvantages
Lithium-ion (Li-ion)	100-250	500-1500	1-3 hours	-20 °C to 60 °C	Medium	High energy density, long cycle life, widely used	Can overheat, degrade over time, safety concerns
Lithium iron phosphate (LiFePO₄)	90-160	2000-5000	1-2 hours	-20 °C to 60 °C	Medium	Very safe, long cycle life, stable performance	Lower energy density than regular Li-ion, bulkier
Nickel-metal Hydride (NiMH)	60-120	500-1000	1-2 hours	-20 °C to 60 °C	Low to medium	Safer than Li-ion, good for low-cost applications	Lower energy density, higher self-discharge rate
Sodium-ion (Na-ion)	90-150	300-400	1-2 hours	-20 °C to 60 °C	Low to medium	Abundant materials, lower cost, safer	Less energy density, shorter cycle span than Li-ion
Zinc-air	300-400	300-500	4-8 hours	0 °C to 60 °C	Low	High energy density, inexpensive, recyclable	Limited cycle life, low power density, and environmental issues
Lead-acid	30-50	200-500	6-12 hours	-20 °C to 50 °C	Low	Very cheap, well-established technology	Very low energy density, large size, short cycle span
Flow batteries (vanadium)	20-40	2000-5000	1-2 hours	-20 °C to 40 °C	High	Scalable, long cycle life, safe	Low energy density, complex design, high cost
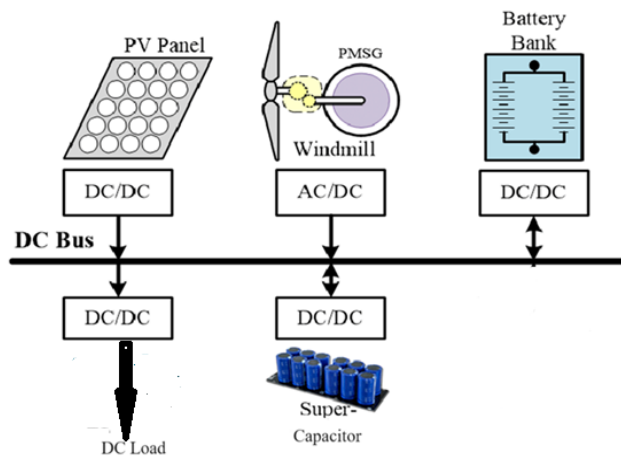
Figure 2. Standard structure of DC microgrid

To address these challenges, a novel multi-source converter topology designed to integrate PV, wind, battery, and ultracapacitor systems more efficiently is proposed, as shown in Figure 3(a). This proposed configuration aims to resolve the issues associated with traditional setups by eliminating the need for dedicated converters and simplifying control mechanisms. It is particularly suitable for DC microgrid applications. The significant advantages of the planned system include: i) the integration of many sources with fewer components, ii) intrinsic voltage enhancing capabilities, iii) built-in voltage control for the ultracapacitor, iv) automatic power allocation between the battery and ultracapacitor, and v) a simplified control system requiring fewer sensors, considered to sustain power balance and optimize maximum power point (MPP) operation for PV and wind sources. The paper is structured as: i) Section 2 explores the system

configuration and operational modes; ii) Section 3 presents the control structure of the proposed system; and iii) Sections 4 and 5 present the key findings and references.

2.   MULTI-SOURCE POWER CONVERTER SETUP

The system arrangement is outlined in Figure 3. Schematic representation is given in Figure 3(a), and along with the converter structure, it is given in Figure 3(b). The proposed microgrid structure includes a PV and HESS connected through a two-way buck-boost DC-DC converter, while wind energy is integrated into the DC link using a DC-DC boost converter. Both PV and wind energy systems are implemented with the perturb and observe MPP tracking algorithm to maximize their output.

The Li-ion battery type is considered in the proposed work, which is available in MATLAB (2018). Lithium-ion batteries have a high energy density, compared to the prominently used lead-acid batteries. Additionally, it has battery capacity, long life, and 80-100% depth of charge. Additionally, they are not toxic to the environment since they use carbon as an anode and lithium salt as a cathode [11]. In this model, the battery is demonstrated as a current source control with internal resistance. The battery gets periodically charged or drained depending on its charge level and the amount of electrical power generated. In this work, the ultracapacitor model is utilized, which is available in MATLAB (2018). The ultracapacitor is modelled as a regulated voltage source with internal resistance. The internal resistance, nominal capacitance, total stored charge, and other variables affect the constraints of the ultracapacitor's operation. System parameter details are given in Table 2.

In this paper battery and ultracapacitor is utilized as HESS. In the proposed multi-source with hybrid energy generating sources key components are the inductors. Lph, Lw, and Lb, which represent the inductances of the PV and hybrid energy storage (HES) converter, wind converter, and HES decoupling inductor, respectively. The PV, battery, ultracapacitor, HESS, wind, and DC bus voltages notations considered are as follows Vpv, Vba, Vs, Vhess, Vw, and Vdc. Current notations are ipv, ilh, iba, isc, iw, and idc, indicating the currents through the PV system, HESS, battery, ultracapacitor, wind system, and DC bus, respectively. Load resistance, internal resistance of battery, and ultracapacitor internal resistance are denoted as Rdc, rb, and rsc. Switches S1 and S2 control the photovoltaic and HES converter, while switches D3 and S4 control the wind converter. Duty cycles for the photovoltaic and HES converter, and wind converter are represented as Dpv and Dw.

When PV power is available, switches S1 and S2 manage the battery charging or discharging and ensure the PV system operates at its MPP. In the absence of PV power, the HESS maintains the voltage across the PV capacitor (Cpv) to normalize the DC bus voltage at the reference value (vdcr) by adjusting S1 and S2. Similarly, switches D3 and S4 control the wind system to achieve MPP operation. The HESS handles the surplus or shortage of power at the DC bus, with the battery managing average power and the ultracapacitor handling oscillatory power. The frequency of current decoupling between the battery and ultracapacitor is influenced by Lb, Csc, rsc, and rb. Based on the power balance principle and buck-boost converter operation mode [28], the following equations are given. When switch S1 is on:

$$V_{ph} = V_{PV} \tag{1}$$

$$V_{dc} = V_{pv} + V_{hess} \tag{2}$$

The (1) and (2) give the status of the system when switch 1 is on. Where V_{ph} is the inductor voltage. When switch S2 is engaged, in this configuration:

$$V_{ph} = V_{hess} \tag{3}$$

$$V_{dc} = V_{pv} + V_{hess} \tag{4}$$

The (3) and (4) give the status of the system when switch 2 is on. This demonstrates that, in both operational modes, the DC-bus voltage is the combined value of the PV and HESS voltages, highlighting the inherent enhancing capability of the planned system. Over a switching period Ts, the steady-state voltage of the HES can be expressed as given in (5).

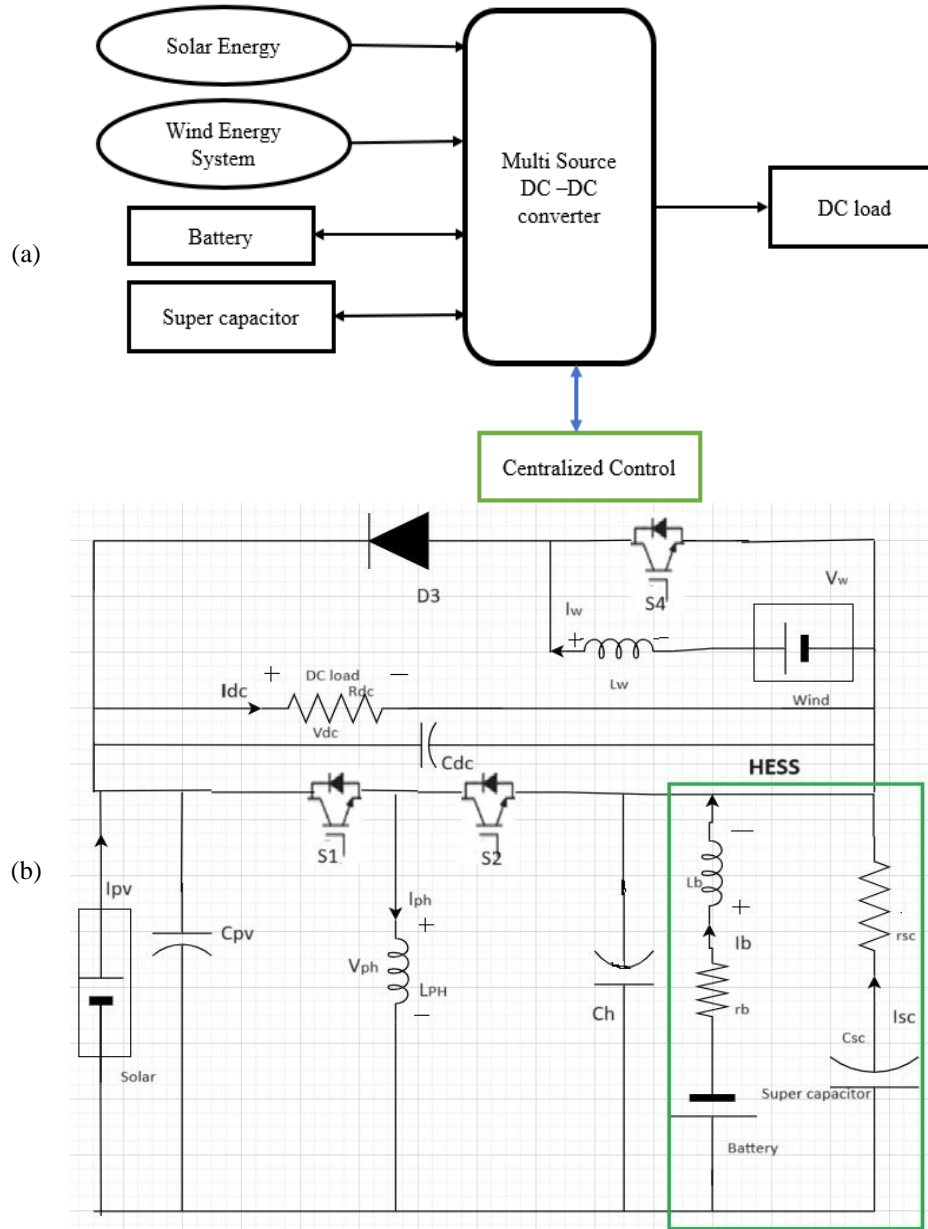$$V_{hess} = \frac{V_{PV}D_{pv}}{1 - D_{PV}V_{PV}} \tag{5}$$

Figure 3. Proposed DC microgrid configuration: (a) schematic diagram of a standalone microgrid with multi-port converter structure and (b) proposed DC microgrid configuration with non-isolated multi-source converter

Similarly, when switches D3 and S4 are active, then the steady-state DC-bus voltage is given by (6).

$$V_{dc} = \frac{D_w}{1-D_W} \tag{6}$$

The steady state condition is given by (7).

$$I_{ph} = I_{hess} + I_{Pv} \tag{7}$$

Thus, both ipv and ihess can be regulated by controlling the inductor current (IPH), particularly when switches S1 and S4 are active while S2 is inactive. The inductors Lph and Lw are charge with current slopes of $\frac{V_{ph}}{L_{ph}}$ and $\frac{V_w}{L_w}$, correspondingly. During this period, capacitor Ch discharges through the HESS, and the load is powered by the DC link capacitor (Cdc). Conversely, when S1 and S4 are inactive and S2 is active, the inductors Lph and Lw discharge through the HESS and the load, respectively. During this time, the PV system delivers power to the load and the DC link capacitor through Lph.

Table 2. Simulation parameters

Sl.No	Categorey	Values	Parameters
1	Wind parameters	Maximum voltage (Vmp)	30 V
		Maximum current (Imp)	3 A
2	PV parameters	Voltage at MPP	17.1 V
		Current at MPP	3.5 A
3	Battery pack	Battery voltage	24 V
		Battery capacity	14 Ah
4	Ultracapacitor pack	Voltage (vsc)	32 V
		Capacitance (Csc)	29 F
5	DC load	resistance	(50-100) Ω
6	Boost converter	components	Lb = 1.99 mH, Lph = 4. 5 mH, Lw = 2 H, Cpv = 2100 µF Ch = 2100 µF, Cw = 1100 µF

3. PROPOSED CONTROL STRATEGY OF MULTI-SOURCE POWER CONVERTER SETUP

The comprehensive control structure is illustrated in Figure 4. The photovoltaic-hybrid energy storage system controller employs a two-loop control system, while the wind control uses a one-loop direct current control system. In the case of the photovoltaic-HESS controller, the inner current controller's reference current is provided by the voltage controller. When PV power is available, the reference PV voltage V_{mp}, obtained from the maximum power point tracking (MPPT) algorithm, is used by the voltage controller as depicted in Figure 4(a). The actual PV voltage is compared to this reference voltage, and the resulting error is processed by a PI controller. The voltage controller then produces a reference current i_{pvr}, which flows through L_{ph} to maintain the PV voltage at V_{mp}. This reference current i_{pvr} is compared with the actual current i_{pv}, and the error is sent to the PI current controller and pulse width generator to create controlling pulses. Figure 4(b) depicts the control structure of the photovoltaic-HESS controller and wind controller control strategy. When PV is not available, the reference voltage (V_{pvr}) for the voltage controller is the difference between the reference DC bus voltage V_{dcr} and the HESS voltage V_{hess} as depicted in Figure 4(b).
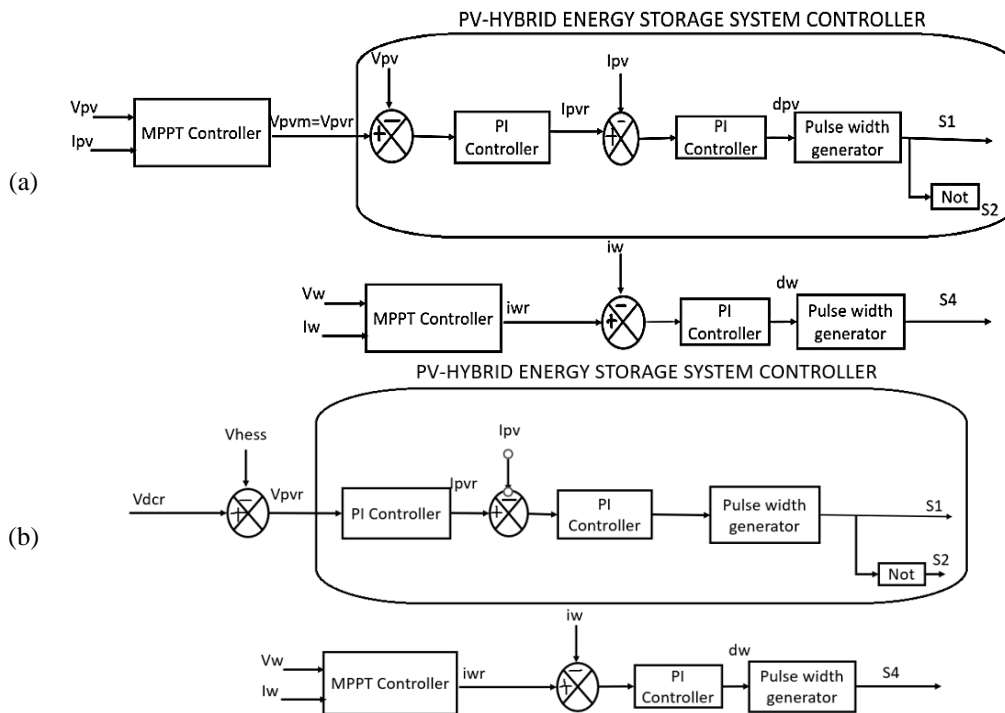

Figure 4. Proposed multi-converter control strategy PV-HESS Controller structure when PV power is (a) available and (b) not available

In the wind control setup, the current produced by the wind MPP algorithm serves as the reference current. The actual wind current i_w is compared to the reference current i_{wr}, and the resultant error is input to a proportional-integral (PI) current controller. The PI controller then determines the necessary duty cycle to

minimize the error. To produce switching pulses, this duty cycle d_{dw} is compared with a high-frequency ramp signal, which sets the converter's switching frequency.

4. RESULTS AND DISCUSSION

In this section, MATLAB/Simulink is utilized to conduct simulations for assessing the performance of the planned system under various operating conditions. The proposed system simulation is given in Figure 5. To test the usefulness of the planned control structure, wind MPP current, irradiance of PV, and load resistance are intentionally changed.
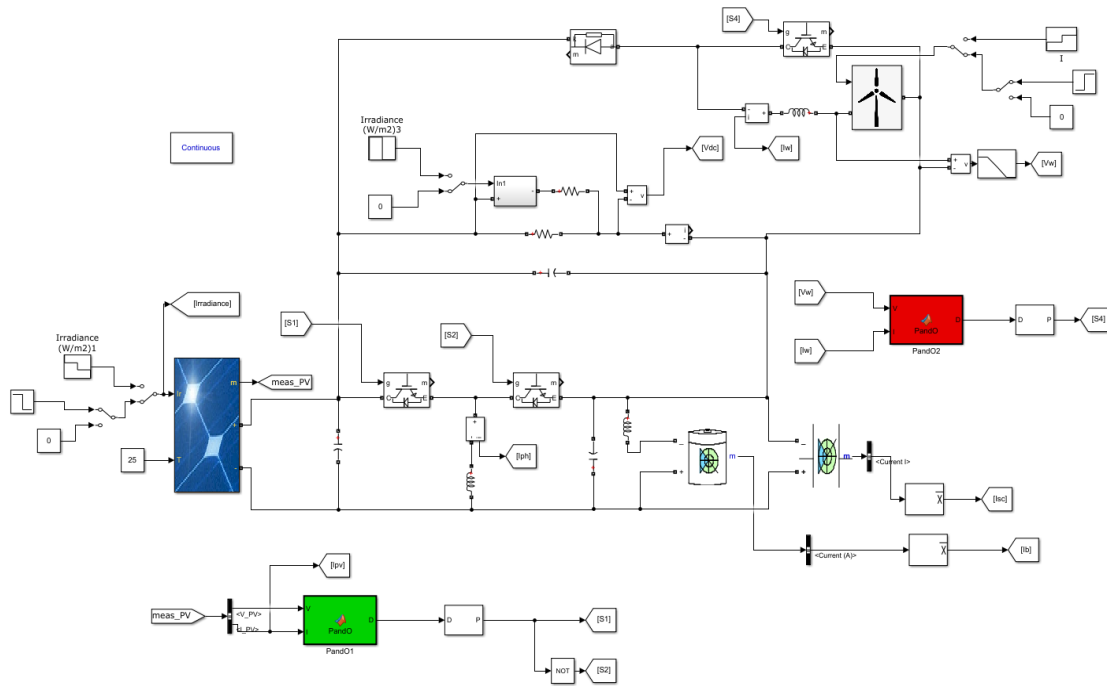
Figure 5. Simulation of the planned DC microgrid with multi-source converters

4.1. With only PV power generation with load variations

The scenario is demonstrated in Figure 6. In this case, solar power is available, but wind power is not. The solar irradiance drops from 1000 W/m² to 500 W/m², causing a decrease in PV current from 2.5 A to 1.5 A, as indicated in the Ipv current curve at t = 2.5 s. Load disturbances are introduced regularly at t = 3 s, t = 5 s, and t = 8 s, as observed from the Iload curve. The DC-bus voltage, depicted in Figure 6, remains stable despite the variations in PV generation and load. Additionally, the ultracapacitor and battery current variations in response to PV power and load power variations are evident from the Isc and Ib curves. It is evident that the ultracapacitor responds to sudden variations while the battery addresses average power requirements.

Consequently, the DC link voltage remains stable at 50 V. In another similar scenario, only the variation in PV generation was analyzed without load variations. This is depicted in Figure 7. In this case, the PV power is available while the wind power is not. The PV power generation decreases at regular intervals, as seen from the Ipv current curve. The DC-link voltage responds to these changes in PV power generation variation, as shown in Figure 7, and remains stable. The Isc and Ib curves, which represent the ultracapacitor and battery current variations in response to PV power generation, also reflect these changes. It is noticed that the ultracapacitor reacts to sudden variations, while the battery responds to average power variations. Therefore, the DC-bus voltage remains stable at 50 V.

4.2. With only wind power generation, with and without load change

This situation is depicted in Figure 8. In this scenario, PV power is not available, while wind power is available. Wind power generation increases at t = 5 s, as shown in the Iw curve, and load disturbances are introduced at regular intervals at t = 3 s, t = 5 s, and t = 8 s. The response of the DC-bus voltage to these changes in wind generation and load variation is visible in Figure 8 and remains stable. Additionally, the Isc and Ib curves, which represent the ultracapacitor and battery current variations in relation to wind power

generation and load variations, show that the ultracapacitor responds to sudden variations, while the battery responds to average power variations. As a result, the DC-bus voltage remains regulated at 50 V.

Figure 9 illustrates the change in wind power generation when there is no variation in load. Additionally, during this scenario, PV power is not available. Wind power generation increases at regular intervals as shown by the wind current curve (Iw). The DC-link voltage, displayed in Figure 9, remains stable in response to these changes in wind generation variation. Additionally, the current variations of the ultracapacitor (Isc) and battery (Ib) in relation to wind power generation are represented in the curves. It is obvious that the ultracapacitor responds to sudden variations while the battery responds to average power variations, ultimately leading to a regulated DC link voltage of 50 V.
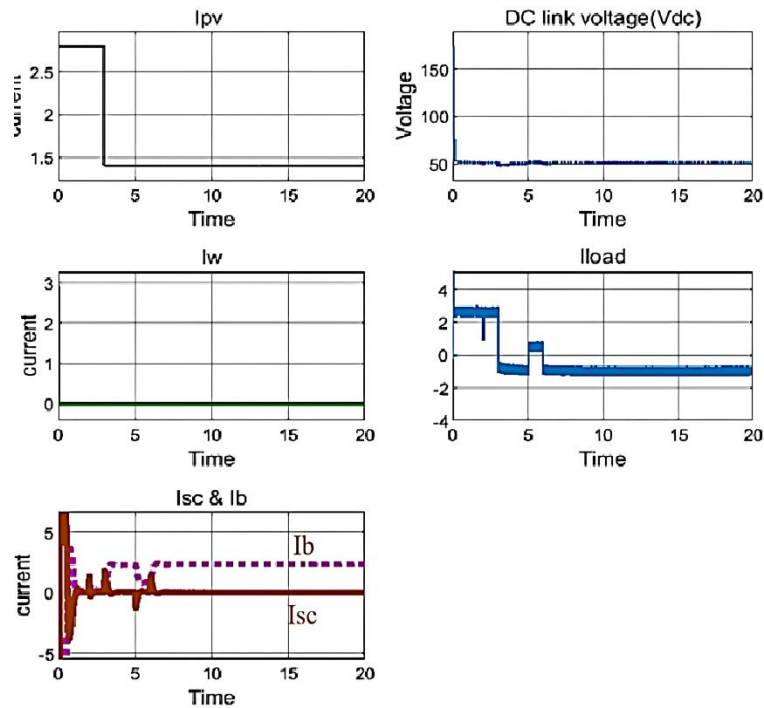

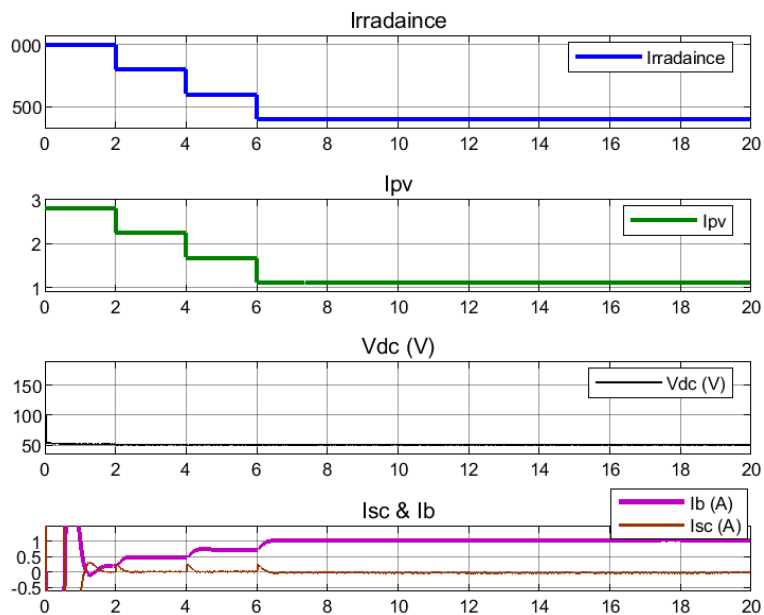Figure 6. With only PV power generation with load variations

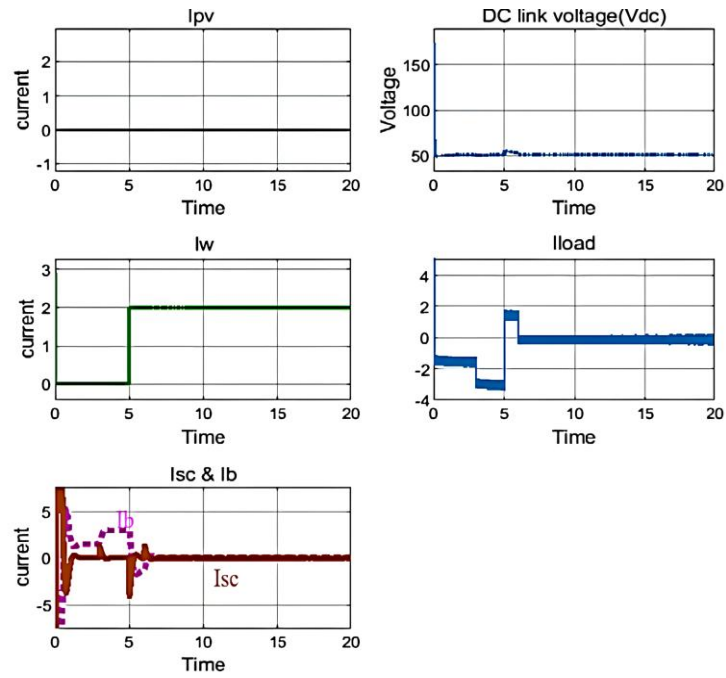Figure 7. With only PV power generation without load variations

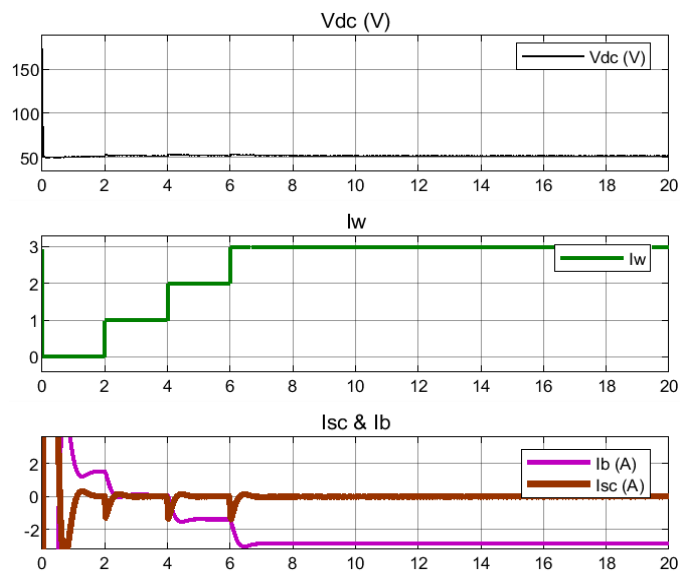Figure 8. With only wind power generation, with load variations

Figure 9. With only wind power generation without load variations

4.3. With only energy storage devices and load variations

This scenario is shown in Figure 10. When neither PV nor wind power is available, the storage unit is responsible for supplying the entire load power. Load variations are evident from the load current curve Iload. Figure 10 illustrates that during disturbances, the ultracapacitor (Isc curve) supplies transient or oscillatory power, while the battery (Ib) provides average or steady-state power. It is also noticeable from the DC link voltage curve that, regardless of these load changes and the absence of generation power, it remains regulated at 50 V.

4.4. PV and wind power generation with and without load variations

The system performance under this scenario is shown in Figure 11. PV, wind, and load disturbances occur at regular intervals during this scenario. Specifically, a PV disturbance is introduced at t = 2.5 s, and a wind disturbance at t = 5 s, and a load disturbance at t = 3 s, t = 5 s, t = 6 s, and t = 8 s. From Figure 11, it is detected from the DC bus voltage curve that the system maintains power balance throughout all disturbances.

The system's performance under PV, wind, and load variation conditions is shown in Figure 12. In this scenario, PV and wind variations occur at regular 2-second intervals until t = 6 s. From the graph in Figure 12, it can be observed that the system maintains power balance throughout all disturbances, and the DC bus voltage remains regulated at 50 V. From the above analyses cases it can be observed that the proposed multi-source performs better in all scenarios compared to the existing microgrid systems with dedicated converters. The elaborate comparison is given in Table 3.
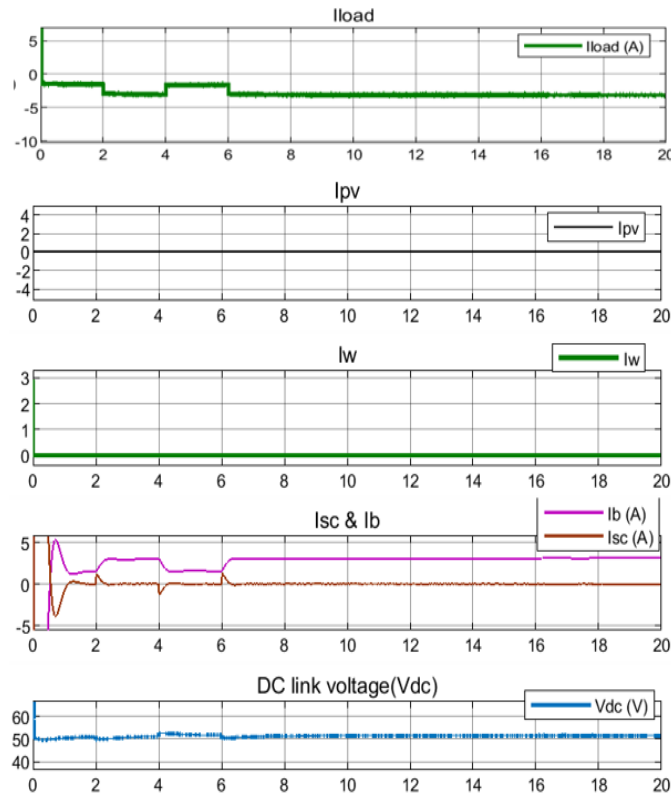

Figure 10. With only energy storage devices with load variations
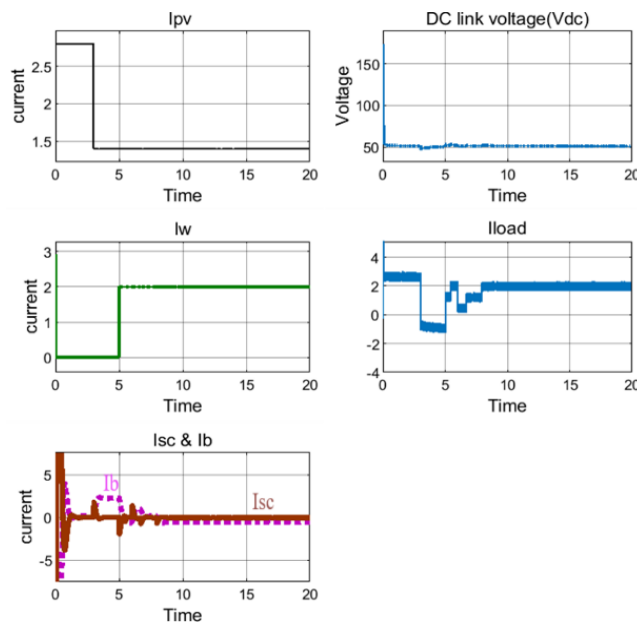

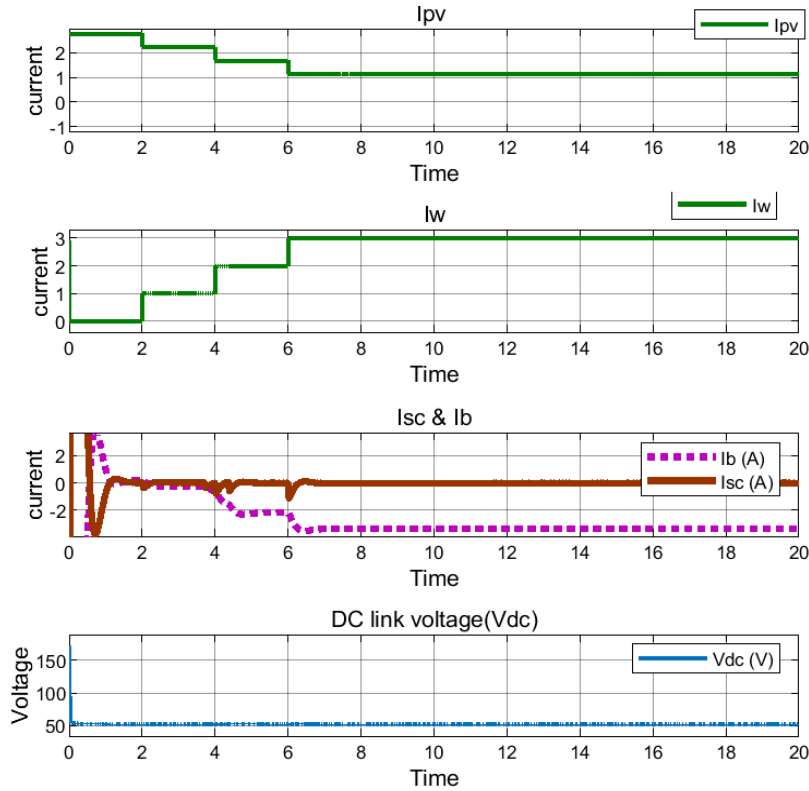Figure 11. PV and wind power generation with load variations

Figure 12. PV and wind power generation with load variations

Table 3. Comparison of a multisource converter-based microgrid with an existing
converter-based microgrid [28]-[30]

Aspect	Multi-port converter-based microgrid	Existing individual DC-DC converter-based microgrid
Number of Switches	Fewer switches -typically, one converter handles all sources (3-8 switches)	More switches -each source/storage has its own converter. (8-20 switches)
Power Stages	Fewer power stages -one multi-port converter handles conversion (1-2 stages)	More power stages -each source/storage has its own converter (2-4 stages)
System Architecture	Centralized architecture with a single converter handling all sources	Decentralized architecture with separate converters for each source/storage
Efficiency	Higher efficiency due to fewer components and conversion stages	Lower efficiency due to multiple conversion stages
Scalability	Limited scalability -restricted by the number of ports in the multi-port converter	Higher scalability -additional converters can be added
Control Complexity	Centralized control, a single controller for all sources	A distributed control converter has its own controller
Cost	Lower cost -fewer converters, switches, and components	Higher cost -more components, converters, and switches
Maintenance	Easier maintenance -monitoring of a single converter	More complex maintenance requires monitoring and repairs of multiple converters
Flexibility	Limited flexibility -restricted by multiport topology	High flexibility -each converter can be customized for specific needs
Application Suitability	Ideal for small to medium systems where simplicity is key	Best suited for large-scale systems requiring flexibility and customization

5. CONCLUSION

Multi-port microgrids provide a highly adaptable and efficient solution for diverse energy needs across various applications, including residential, industrial, military, and remote locations. By integrating solar and wind with battery and ultracapacitor storage, these systems offer flexibility to meet dynamic energy demands. As the worldwide focus moves toward more sustainable and resilient energy solutions, multi-port microgrids are set to play a significant role in providing clean, efficient, and cost-effective power solutions across different sectors. The newly developed multi-source converter design for integrating PV systems, wind turbines, and HESS has shown promising performance. Through thorough analysis, modelling, and simulation, the system demonstrated effective management of renewable energy sources, maintaining MPPT for both PV and wind systems, and efficiently managing energy storage charging/discharging. The

ultracapacitor played a crucial role in reducing battery stress and smoothing out fluctuations caused by intermittent renewable power and sudden load changes.

Especially, the proposed setup stands out due to its reduced number of switches, inherent voltage boosting capabilities, and resourceful power allocation between the battery and ultracapacitor. These features, along with the fewer required sensors, make this design more cost-effective and simpler than traditional configurations. Further research into protection schemes and real-world testing could enhance the robustness and reliability of this innovative configuration.

FUNDING INFORMATION

AUTHOR CONTRIBUTIONS STATEMENT

This journal uses the Contributor Roles Taxonomy (CRediT) to recognize individual author contributions, reduce authorship disputes, and facilitate collaboration.

Name of Author	C	M	So	Va	Fo	I	R	D	O	E	Vi	Su	P	Fu
Suganthi Neelagiri	✓	✓	✓	✓	✓	✓		✓	✓	✓			✓	
Pasumarthi Usha		✓			✓				✓	✓				

C : **C**onceptualization	I : **I**nvestigation	Vi : **Vi**sualization
M : **M**ethodology	R : **R**esources	Su : **Su**pervision
So : **So**ftware	D : **D**ata Curation	P : **P**roject administration
Va : **Va**lidation	O : Writing - **O**riginal Draft	Fu : **Fu**nding acquisition
Fo : **Fo**rmal analysis	E : Writing - Review & **E**diting	

CONFLICT OF INTEREST STATEMENT

Authors state no conflict of interest.

DATA AVAILABILITY

Data availability is not applicable to this paper as no new data were created or analyzed in this study.

REFERENCES

[1] A. A. Al Alahmadi *et al.*, "Hybrid wind/PV/battery energy management-based intelligent non-integer control for smart DC-microgrid of smart university," *IEEE Access*, vol. 9, pp. 98948–98961, 2021, doi: 10.1109/ACCESS.2021.3095973.

[2] T. Skrúcaný, M. Kendra, O. Stopka, S. Milojević, T. Figlus, and C. Csiszár, "Impact of the electric mobility implementation on the greenhouse gases production in Central European countries," *Sustainability*, vol. 11, no. 18, p. 4948, Sep. 2019, doi: 10.3390/su11184948.

[3] A. Merabet, K. Tawfique Ahmed, H. Ibrahim, R. Beguenane, and A. M. Y. M. Ghias, "Energy management and control system for laboratory scale microgrid based wind-PV-battery," *IEEE Transactions on Sustainable Energy*, vol. 8, no. 1, pp. 145–154, Jan. 2017, doi: 10.1109/TSTE.2016.2587828.

[4] Z. Šimić, D. Topić, G. Knežević, and D. Pelin, "Battery energy storage technologies overview," *International Journal of Electrical and Computer Engineering Systems*, vol. 12, no. 1, pp. 53–65, Apr. 2021, doi: 10.32985/ijeces.12.1.6.

[5] C. R. Arunkumar, U. B. Manthati, and S. Punna, "Supercapacitor voltage-based power sharing and energy management strategy for hybrid energy storage system," *Journal of Energy Storage*, vol. 50, p. 104232, Jun. 2022, doi: 10.1016/j.est.2022.104232.

[6] T. Sutikno, W. Arsadiando, A. Wangsupphaphol, A. Yudhana, and M. Facta, "A review of recent advances on hybrid energy storage system for solar photovoltaics power generation," *IEEE Access*, vol. 10, pp. 42346–42364, 2022, doi: 10.1109/ACCESS.2022.3165798.

[7] N. C. Alluraiah and P. Vijayapriya, "Optimization, design, and feasibility analysis of a grid-integrated hybrid ac/dc microgrid system for rural electrification," *IEEE Access*, vol. 11, pp. 67013–67029, 2023, doi: 10.1109/ACCESS.2023.3291010.

[8] A. Khaligh and Zhihao Li, "Battery, ultracapacitor, fuel cell, and hybrid energy storage systems for electric, hybrid electric, fuel cell, and plug-in hybrid electric vehicles: state of the art," *IEEE Transactions on Vehicular Technology*, vol. 59, no. 6, pp. 2806–2814, Jul. 2010, doi: 10.1109/TVT.2010.2047877.

[9] A. Kachhwaha *et al.*, "Design and performance analysis of hybrid battery and ultracapacitor energy storage system for electrical vehicle active power management," *Sustainability*, vol. 14, no. 2, p. 776, Jan. 2022, doi: 10.3390/su14020776.

[10] M. E. Şahin and F. Blaabjerg, "A hybrid PV-battery/supercapacitor system and a basic active power control proposal in MATLAB/Simulink," *Electronics*, vol. 9, no. 1, p. 129, Jan. 2020, doi: 10.3390/electronics9010129.

[11] B. Boubaker, T. Mustapha, and K. Houari, "Hybrid storage system energy management based on a predictive current controller," *International Journal on Energy Conversion (IRECON)*, vol. 6, no. 4, p. 121, Jul. 2018, doi: 10.15866/irecon.v6i4.15790.

[12] J. Lu, W. Zheng, Z. Yu, Z. Xu, H. Jiang, and M. Zeng, "Optimizing grid-connected multi-microgrid systems with shared energy storage for enhanced local energy consumption," *IEEE Access*, vol. 12, pp. 13663–13677, 2024, doi: 10.1109/ACCESS.2024.3351855.

[13] M. Yadav, N. Pal, and D. K. Saini, "Microgrid control, storage, and communication strategies to enhance resiliency for survival of critical load," *IEEE Access*, vol. 8, pp. 169047–169069, 2020, doi: 10.1109/ACCESS.2020.3023087.

[14] U. Subramaniam, S. Vavilapalli, S. Padmanaban, F. Blaabjerg, J. B. Holm-Nielsen, and D. Almakhles, "A hybrid PV-battery system for ON-grid and OFF-grid applications—controller-in-loop simulation validation," *Energies*, vol. 13, no. 3, p. 755, Feb. 2020, doi: 10.3390/en13030755.

[15] T. Sutikno, A. S. Samosir, R. A. Aprilianto, H. S. Purnama, W. Arsadiando, and S. Padmanaban, "Advanced DC–DC converter topologies for solar energy harvesting applications: a review," *Clean Energy*, vol. 7, no. 3, pp. 555–570, Jun. 2023, doi: 10.1093/ce/zkad003.

[16] M. Faisal, M. A. Hannan, P. J. Ker, A. Hussain, M. Bin Mansor, and F. Blaabjerg, "Review of energy storage system technologies in microgrid applications: issues and challenges," *IEEE Access*, vol. 6, pp. 35143–35164, 2018, doi: 10.1109/ACCESS.2018.2841407.

[17] M. Ahmed, S. Kuriry, M. D. Shafiullah, and M. A. Abido, "DC microgrid energy management with hybrid energy storage systems," in *2019 23rd International Conference on Mechatronics Technology (ICMT)*, IEEE, Oct. 2019, pp. 1–6. doi: 10.1109/ICMECT.2019.8932147.

[18] S. K. Kollimalla, M. K. Mishra, A. Ukil, and H. B. Gooi, "DC grid voltage regulation using new HESS control strategy," *IEEE Transactions on Sustainable Energy*, vol. 8, no. 2, pp. 772–781, Apr. 2017, doi: 10.1109/TSTE.2016.2619759.

[19] S. K. Kollimalla, A. Ukil, H. B. Gooi, U. Manandhar, and N. R. Tummuru, "Optimization of charge/discharge rates of a battery using a two-stage rate-limit control," *IEEE Transactions on Sustainable Energy*, vol. 8, no. 2, pp. 516–529, Apr. 2017, doi: 10.1109/TSTE.2016.2608968.

[20] S. Tyagi, B. Singh, and S. Das, "Control of interlinking converter for power quality improvement in hybrid microgrid," *IEEE Transactions on Industrial Electronics*, vol. 72, no. 2, pp. 1607–1616, Feb. 2025, doi: 10.1109/TIE.2024.3419224.

[21] X. Liu, T. Zhao, H. Deng, P. Wang, J. Liu, and F. Blaabjerg, "Microgrid energy management with energy storage systems: a review," *CSEE Journal of Power and Energy Systems*, vol. 9, no. 2, pp. 483–504, 2023, doi: 10.17775/CSEEJPES.2022.04290.

[22] P. S. Kumar, R. P. S. Chandrasena, V. Ramu, G. N. Srinivas, and K. V. S. M. Babu, "Energy management system for small scale hybrid wind solar battery based microgrid," *IEEE Access*, vol. 8, pp. 8336–8345, 2020, doi: 10.1109/ACCESS.2020.2964052.

[23] N. Suganthi and P. Usha, "Control of microgrid with hybrid energy storage system," in *International Conference on Power, Control, and Sustainable Energy Systems*, River Publishers Series in Proceedings, 2023, pp. 1–345. doi: 10.13052/rp-9788770229630.

[24] C. B. Ndeke, M. Adonis, and A. Almaktoof, "Energy management strategy for a hybrid micro-grid system using renewable energy," *Discover Energy*, vol. 4, no. 1, Feb. 2024, doi: 10.1007/s43937-024-00025-9.

[25] U. Manandhar, N. R. Tummuru, S. K. Kollimalla, A. Ukil, G. H. Beng, and K. Chaudhari, "Validation of faster joint control strategy for battery- and supercapacitor-based energy storage system," *IEEE Transactions on Industrial Electronics*, vol. 65, no. 4, pp. 3286–3295, Apr. 2018, doi: 10.1109/TIE.2017.2750622.

[26] Q. Xu, J. Xiao, P. Wang, X. Pan, and C. Wen, "A decentralized control strategy for autonomous transient power sharing and state-of-charge recovery in hybrid energy storage systems," *IEEE Transactions on Sustainable Energy*, vol. 8, no. 4, pp. 1443–1452, Oct. 2017, doi: 10.1109/TSTE.2017.2688391.

[27] D. Marinković, G. Dezső, and S. Milojević, "Application of machine learning during maintenance and exploitation of electric vehicles," *Advanced Engineering Letters*, vol. 3, no. 3, pp. 132–140, 2024, doi: 10.46793/adeletters.2024.3.3.5.

[28] J. Narayanaswamy and S. Mandava, "Non-isolated multiport converter for renewable energy sources: a comprehensive review," *Energies*, vol. 16, no. 4, p. 1834, Feb. 2023, doi: 10.3390/en16041834.

[29] P. Kolahian, H. Tarzamni, A. Nikafrooz, and M. Hamzeh, "Multi-port DC–DC converter for bipolar medium voltage DC micro-grid applications," *IET Power Electronics*, vol. 12, no. 7, pp. 1841–1849, Jun. 2019, doi: 10.1049/iet-pel.2018.6031.

[30] B. S. Revathi and P. Mahalingam, "Hybrid modular converter for DC microgrids," *IET Power Electronics*, vol. 11, no. 5, pp. 856–865, May 2018, doi: 10.1049/iet-pel.2016.1034.

BIOGRAPHIES OF AUTHORS

Suganthi Neelagiri received the bachelor's degree in Electrical and Electronics Engineering from Bharathiyar University in 2001, the master's degree in Electrical Power and Energy System from Uttara Pradesh Technical University in 2013, and Ph.D. in Electrical Engineering from Visvesvaraya University, respectively. She is currently working as an Assistant Professor at the Department of Electrical and Electronics Engineering, Dayananda Sagar College of Engineering. Her research areas include microgrids, renewable energy systems, and energy storage systems. She can be contacted at email: suganthi_neelagiri@yahoo.com.

Pasumarthi Usha received the bachelor's degree in Electrical and Electronics from J.N.T.U, College of Engineering Kakinada in 1990, the master's degree in Power System with emphasis in High Voltage from J.N.T.U, College of Engineering Kakinada in 1992, and the Ph.D. in HVDC Power Transmission from Visvesvaraya Technical University in 2013, respectively. She is currently working as a Professor at the Department of Electrical and Electronics Engineering, Dayananda Sagar College of Engineering. Her research areas include HVDC power systems, microgrids, and power electronics. She can be contacted at email: pu1968@yahoo.co.in.